J Solid State Electrochem (2001) 5: 88–93

ORIGINAL PAPER

Frank Marken · Richard G. Compton
Christiaan H. Goeting · John S. Foord
Steven D. Bull · Stephen G. Davies

Fast electrochemical triple-interface processes at boron-doped diamond electrodes

Received: 3 February 2000 / Accepted: 18 February 2000

Abstract Two important mechanisms for electron transfer processes at boron-doped diamond electrodes involving the oxidation of tetramethylphenylenediamine (TMPD) dissolved in aqueous solution and the oxidation of tetrahexylphenylenediamine (THPD) deposited in the form of microdroplets and immersed into aqueous eletrolyte solution are reported. For TMPD, the first oxidation step in aqueous solution follows the equation:

$$TMPD_{aqueous} \rightleftharpoons TMPD^{+}_{aqueous} + e^{-}$$

Remarkably slow heterogeneous kinetics at a H-plasma-treated boron-doped diamond electrode are observed, consistent with a process following a pathway more complex than outer-sphere electron transfer. At the same boron-doped diamond electrode surface a deposit of THPD undergoes facile oxidation following the equation:

$$THPD_{organic} + SCN^{-}_{aqueous} \rightleftharpoons [THPD^{+}SCN^{-}]_{organic} + e^{-}$$

This oxidation and re-reduction of the deposited liquid material occurs at the triple interface organic droplet|diamond|aqueous electrolyte and is therefore an example of a facile high-current-density process at boron-doped diamond electrodes due to good electrical contact between the deposit and the diamond surface.

Key words Boron-doped diamond · Modified electrodes · Ionic liquids · Triple phase boundary · Voltammetry

F. Marken (✉) · R.G. Compton · C.H. Goeting · J.S. Foord
Physical and Theoretical Chemistry Laboratory,
Oxford University, Oxford OX1 3QZ, UK
e-mail: frank@physchem.ox.ac.uk

S.D. Bull · S.G. Davies
Dyson Perrins Laboratory, Oxford University,
Oxford OX1 3QY, UK

Introduction

Electrochemical processes at synthetic highly boron-doped diamond electrodes have attracted considerable attention over recent years [1–3] and have been successfully studied in conjunction with several applications in electrosynthesis [4, 5] and electroanalytical detection [6, 7]. Properties of diamond electrodes such as chemical inertness, a wide potential window, and low interfacial capacity (low background currents) have been exploited in analytical processes [8, 9] and in realising high-overpotential processes such as ozone generation [10], organic waste destruction [11], and total nitrate reduction [12].

Complex electrochemical processes at the boron-doped diamond|solution (electrolyte) interface are often found to occur with a slow rate compared to similar processes at other types of carbon or metal electrode surfaces. The wide potential window accessible at boron-doped diamond electrodes and the formation of chlorine, bromine, and iodine are typical examples [13, 14]. Furthermore, the state of the surface of the diamond has been shown to be crucial in governing the reactivity (e.g. see [15]). For example, the rate of oxygen reduction at boron-doped diamond electrodes is affected strongly by the history of the electrode surface [16].

Electrochemically formed metal deposits on boron-doped diamond electrodes have been studied by several groups [17–20]. The cathodic deposition of Pb and Ag have been shown to follow a nucleation and growth type mechanism and a slow anodic "stripping" with a characteristic tailing has been observed and attributed to weak adhesion or interaction between the deposit and the electrode [19, 20]. On the other hand, achieving good adhesion and facile electron transfer between the diamond electrode surface and deposit may provide the key to a novel type of modified electrode with an "inert" substrate, boron-doped diamond, and a selective electrocatalyst chemically attached or deposited. Details concerning the reactivity of the boron-doped diamond

electrode surface towards deposited materials are therefore of considerable importance.

In the present work it is shown that, after the problem of good adhesion has been solved, highly boron-doped diamond electrodes are ideal substrate materials for applications as modified electrodes. A model system, the oxidation and re-reduction of tetrahexylphenylenediamine (THPD) [21], is used as a deposit on boron-doped diamond. THPD is a liquid redox system which is known to undergo reversible oxidation accompanied by anion insertion without dissolution in the surrounding aqueous solution phase [22] (Eq. 1):

$$\mathrm{THPD_{organic}} + [\mathrm{X^-}]_{\mathrm{aqueous}} \rightleftharpoons [\mathrm{THPD^+X^-}]_{\mathrm{organic}} + \mathrm{e^-} \quad (1)$$

In this equation, X^- denotes an anion such as ClO_4^-, PF_6^-, or SCN^-. The liquid nature of the electroactive deposit facilitates good interaction of the deposit with the electrode surface. It is shown that THPD deposited on a boron-doped diamond electrode surface undergoes facile redox conversion via a three-phase boundary process with extremely high local current density. In contrast to this, the analogous solution phase oxidation of tetramethylphenylenediamine (TMPD) is shown to proceed with unusually slow kinetics.

Experimental

Chemicals

THPD was prepared as described previously [21]. TMPD was used in the form of the dihydrochloride (Aldrich). KSCN and KCl (both Aldrich) were purchased in the purest commercially available grade and used without further purification. A solvent evaporation method employing a solution of 1 mM THPD in acetonitrile (dried and distilled, Fisons) was used for the deposition of THPD on electrode surfaces. Deionised water was taken from an Elgastat filter system (Elga, Bucks, UK) with a resistivity of not less than 18 MΩ cm. Argon (Pureshield, BOC, UK) was used for degassing solutions prior to electrochemical measurements. All experiments were conducted at a temperature of 20 ± 2 °C.

Instrumentation

A standard three-electrode electrochemical cell with a platinum counter electrode, a saturated calomel reference electrode (SCE, Radiometer Kopenhagen), and working electrode were used. The working electrode was a 4.9 mm diameter basal-plane pyrolytic graphite disc or a 5 × 5 × 0.6 mm polycrystalline diamond plate. The polycrystalline boron-doped diamond working electrode (DeBeers Industrial Diamonds, Berks, UK) consisted of a free-standing film with a crystal size of typically 10–50 μm (see Fig. 1a) and was low-temperature H-plasma treated [23] and fitted into a Teflon holder. The boron-doping level ($1.2–1.5 \times 10^{20}$ cm^{-3}) was determined by Raman spectroscopy [24], based on the characteristic signals at 500, 1200, and 1330 cm^{-1} (see Fig. 2). Voltammetric measurements were performed with a PGSTAT 20 AUTOLAB system (Eco Chemie, Netherlands). SEM images were obtained with a JEOL JSM 5200 system and a 2 h low-temperature H-plasma treatment (25–70 °C, 320 W RF-plasma, 4 mbar hydrogen) was used for cleaning and conditioning the surface of the boron-doped diamond [23]. A Dilor Labram spectrometer with a He-Ne 20 mW laser (632.817 nm) was employed for Raman analysis.

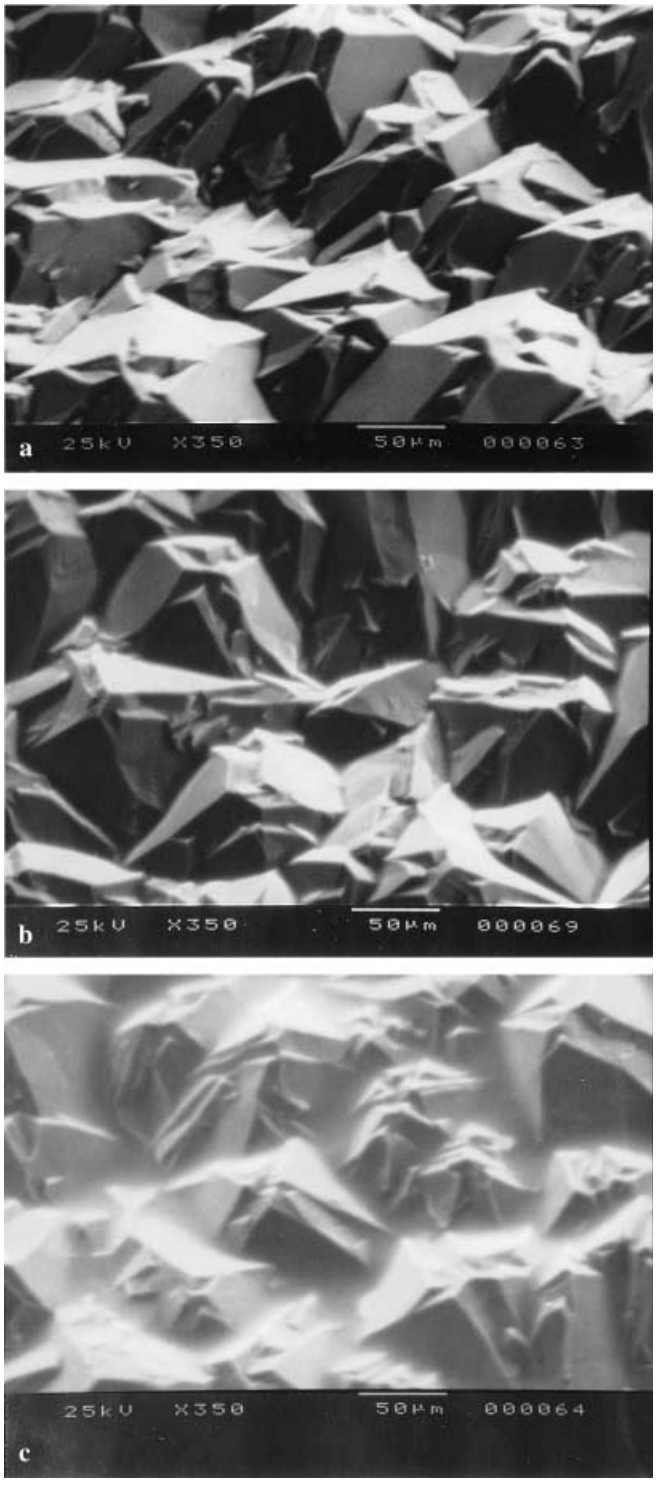

Fig. 1 SEM images of **a** a polycrystalline boron-doped diamond electrode surface, **b** with 3 μg THPD deposited and electrochemically oxidised to $[\mathrm{THPD^+SCN^-}]_{\mathrm{organic}}$, and **c** with 30 μg THPD deposited and electrochemically oxidised to $[\mathrm{THPD^+SCN^-}]_{\mathrm{organic}}$

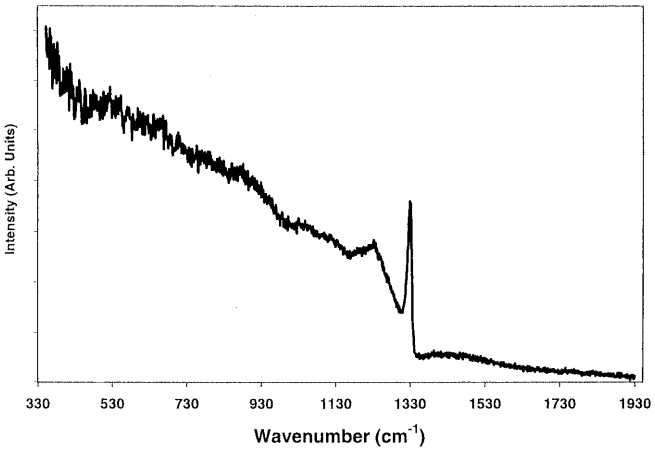

Fig. 2 Raman spectrum for the H-plasma-treated polycrystalline boron-doped diamond electrode

Results and discussion

Oxidation of TMPD dissolved in aqueous solution

Boron-doped diamond has been proposed as a versatile electrode material with voltammetric characteristics related/superior to those of glassy carbon or other types of carbon [20] and with electrochemical properties strongly dependent on both the level of boron doping [24] and the surface treatment [25]. The characteristics of diamond electrodes employed here have been reported recently [16]. The electrode obtained after H-plasma treatment allows well-defined voltammetric responses, e.g. for typical outer-sphere one-electron transfer processes such as the reduction of $Ru(NH_3)_6^{3+}$ in aqueous 0.1 M KCl, to be obtained [16, 23].

The oxidation of TMPD is known to proceed stepwise in two reversible one-electron transfer processes in aqueous solution [26–28]. In Fig. 3a, cyclic voltammograms obtained for a solution of 1 mM TMPD in aqueous 0.2 M KCl obtained at a 4.9 mm diameter basal-plane pyrolytic graphite electrode are shown. The two processes observed at $E_{1/2} = 0.22$ V vs. SCE and at $E_{1/2} = 0.44$ V vs. SCE may be attributed to processes described in the following two equations:

$$TMPD_{aqueous} \rightleftharpoons TMPD^{+}_{aqueous} + e^{-} \quad (2)$$

$$TMPD^{+}_{aqueous} \rightleftharpoons TMPD^{2+}_{aqueous} + e^{-} \quad (3)$$

For both processes shown in Fig. 3a, well-defined diffusion-controlled voltammetric responses are observed with a peak current proportional to the square root of the scan rate. The peak-to-peak separation observed for the first oxidation process, $\Delta E = 82$ mV, is slightly wider than that for the second oxidation process, $\Delta E = 64$ mV. In Fig. 3b, cyclic voltammograms for the oxidation of 1 mM TMPD at a 5×5 mm polycrystalline highly boron-doped diamond electrode are shown. It can be seen that the first redox wave corresponding to

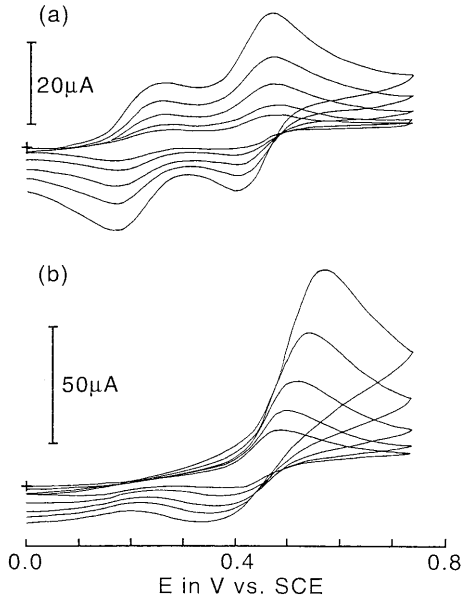

Fig. 3 Cyclic voltammograms obtained for the oxidation of 1 mM TMPD in aqueous 0.2 M KCl at a scan rates of 20, 50, 100, and 200 mV s^{-1}: **a** at a 4.9 mm diameter basal-plane pyrolytic graphite electrode and **b** at a 5×5 mm polycrystalline boron-doped diamond electrode

the process given in Eq. 1 appears to be suppressed under these conditions. This oxidation is now detected in the form of a shoulder at ca. 0.4 V vs. SCE. Also, the reduction associated with the process given in Eq. 2 is slow and may be assigned to the small and scan-rate-dependent responses at ca. 0.1 V vs. SCE. The second redox process for the oxidation of $TMPD^{+}$ to $TMPD^{2+}$ on diamond appears to proceed with a considerably faster rate and, owing to the slow first oxidation step, is effectively two electron in nature. At a scan rate of 200 mV s^{-1} the current density at the peak for the one-electron oxidation at the basal-plane pyrolytic graphite electrode (Fig. 3a) is 202 μA cm^{-2}, which may be compared to a current density of 374 μA cm^{-2} for the second oxidation process at the boron-doped diamond electrode. The comparison of the peak current densities confirms the proposed two-electron transfer at diamond following Eqs. 2, 3, and 4:

$$TMPD^{2+}_{aqueous} + TMPD_{aqueous} \rightleftharpoons 2TMPD^{+}_{aqueous} \quad (4)$$

The mechanistic details responsible for the peculiar voltammetric characteristics observed for the first oxidation of TMPD at a boron-doped diamond surface are at the moment not understood in detail but are probably related to the observation of "complex" redox processes occurring with a slow rate at boron-doped diamond electrodes [14]. Furthermore, the flat-band potential for boron-doped diamond electrode surfaces with H-termination has been reported to be in the range 0.5–1.0 V vs. SCE [2]. The voltammetric responses shown in Fig. 3b could be explained by a change of the electrochemical characteristics of the diamond surface near the

flat-band potential, positive of which p-type semiconductors would be expected to conduct. However, this effect is not detected for other redox couples, such as $Ru(NH_3)_6^{3+}$, even at more negative potentials and is therefore a manifestation of the interaction between the diamond surface and the dissolved redox reagent.

Oxidation of THPD deposited in the form of microdroplets

It is very interesting to compare the redox behaviour of compounds dissolved in the aqueous solution phase with structurally closely related but insoluble materials deposited onto the electrode surface and immersed into the aqueous electrolyte solution. Understanding the interaction of the deposit and the electrode surface and the nature of the electron transfer process is important for the development of new types of modified electrodes and novel processes such as organic/aqueous emulsion electrolysis [29].

Electrochemical processes involving selective anion uptake into an organic deposit of THPD adhered to a basal-plane pyrolytic graphite electrode have recently been shown [20, 21, 30] to occur upon oxidation of the organic material in the presence of a suitable aqueous electrolyte. The process was characterised in the presence of aqueous 0.1 M KSCN as a bulk one-electron oxidation with a stoichiometry given by Eq. 5:

$$THPD_{organic} + [SCN^-]_{aqueous} \rightleftharpoons [THPD^+SCN^-]_{organic} + e^- \quad (5)$$

The THPD deposit has been shown to be in the form of an array of microdroplets of an electroactive organic oil of ca. 1–10 μm size. After redox conversion the product, $[THPD^+SCN^-]_{organic}$, remains in a liquid state with anions, SCN^-, able to undergo rapid exchange with the solution phase [22]. In Fig. 4a, typical voltammograms obtained with various amounts of THPD deposited onto a basal-plane pyrolytic graphite electrode and immersed in aqueous 0.1 M SCN^- are shown for scan rates of 20 mV s^{-1}. The voltammetric response at $E_{1/2} = 0.18$ V vs. SCE has the characteristics of a reversible surface-confined redox system with, at low coverage and low scan rates, a linear dependence of the peak current and the scan rate. For an amount of 0.3 μg THPD deposited, the expected charge for a quantitative one-electron conversion can be calculated as $Q = 66$ μC. A series of cyclic voltammograms obtained for increasing amounts of THPD deposit are shown. The peak-to-peak separation (see Table 1) becomes very small, especially for small amounts of deposit and slow scan rates. The second oxidation process in the presence of aqueous electrolyte (not shown) is accompanied by irreversible chemical steps, possibly involving the cleavage of the C-N bond (e.g. see [31]) and is not considered in this study.

The region in which the electrochemical process for microdroplet deposits occurs has been shown to be consistent with the triple interface THPD deposit|electrode|aqueous electrolyte [32]. Current densities arising at the triple interface can be substantial and, for the case of electrochemical processes of deposits on boron-doped diamond, problems due to high current density may be predicted. In the voltammogram shown in Fig. 3b a peak current of 50 μA corresponds to a current density

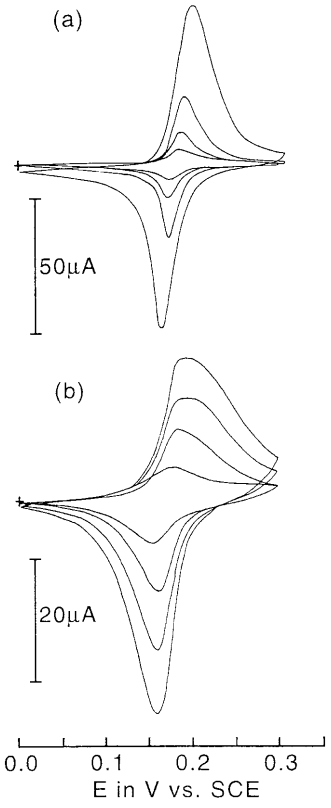

Fig. 4 Cyclic voltammograms obtained for the oxidation of microdroplet deposits of THPD (0.3, 0.6, 1.5, and 3 μg) in aqueous 0.1 M KSCN at a scan rate of 20 mV s^{-1}: **a** at a 4.9 mm diameter basal-plane pyrolytic graphite electrode and **b** at a 5 × 5 mm polycrystalline boron-doped diamond electrode

Table 1 Voltammetric data for the oxidation of THPD deposited onto the electrode surface and immersed in aqueous 0.1 M KSCN at a 4.9 mm diameter basal-plane pyrolytic graphite electrode and at a 5 × 5 mm polycrystalline H-plasma-treated boron-doped diamond electrode

THPD deposit (μg)	E_p^{ox} (V vs. SCE)	I_p^{ox} (μA)	E_p^{red} (V vs. SCE)	I_p^{red} (μA)	Q^a (μC)
4.9 mm diameter basal-plane pyrolytic graphite					
0.3	0.182	5.6	0.171	−5.4	20
0.6	0.183	12	0.170	−12	30
1.5	0.187	26	0.170	−26	56
3.0	0.195	60	0.163	−61	163
5 × 5 mm polycrystalline boron-doped diamond					
0.3	0.176	5.4	0.156	−7.4	34
0.6	0.187	11	0.161	−15	55
1.5	0.192	17	0.160	−24	92
3.0	0.190	23	0.158	−35	127

[a] Charge calculated by integration over the voltammetric response

of ca. 200 μA cm^{-2} based on the geometric area of the electrode. In contrast, an estimate for the triple-phase boundary area for a droplet deposit of 1 μm radius semispheres with a 10 nm effective width of the triple interface amounts to an interfacial area a factor 1000 less than the geometric area. Therefore current densities three orders of magnitude or more *higher* can be anticipated. For the case of metal particles deposited on boron-doped diamond electrodes, it has been shown that electron transfer can be slow owing to high current densities and insufficient electrical contact [19, 20].

In Fig. 4b, cyclic voltammograms for the oxidation and re-reduction of various amounts of THPD deposited onto the diamond surface with a scan rate of 20 mV s^{-1} are shown. The voltammetric responses show very similar characteristics compared to those observed at basal-plane pyrolytic graphite (Fig. 4a). The peak shape, which is strongly dependent on the size of the droplet deposit [21, 22], is slightly broader; however, the peak-to-peak separation is small and, especially at low coverage of the electrode surface, integration of the current response suggests nearly complete conversion. Therefore facile electron transfer between the liquid deposit and the boron-doped diamond electrode surface is possible even at high current density. The "wetting" of the hydrophobic H-terminated diamond surface appears to provide good electrical contact.

The oxidised form of the deposit, $[THPD^+SCN^-]_{organic}$, behaves like an ionic liquid and remains non-volatile even under vacuum conditions. SEM images for the oxidised deposit on polycrystalline diamond are shown in Fig. 1b and c. Perhaps surprisingly, initially the deposit was very difficult to detect. Only by increasing the amount of deposit from 0.3 μg to 30 μg can a "haze" be detected, consistent with material present especially between the diamond crystals. The same although weaker effect indicates the presence of the deposit in Fig. 1b. Electrons appear to be able to penetrate into the liquid deposit to some extent. After cleaning the sample shown in Fig. 1c with acetonitrile, an SEM similar to that shown in Fig. 1a was observed.

Conclusions

For the case of TMPD and THPD oxidation at boron-doped diamond electrodes, two interesting and potentially important experimental findings have been reported. The first oxidation step of TMPD dissolved in aqueous solution can be observed to proceed with very slow kinetics at H-plasma-treated boron-doped diamond electrodes and therefore TMPD may be regarded as a model system for further studies into the nature of the kinetic selectivity observed at diamond electrodes. Second, the first oxidation step of THPD deposited in the form of microdroplets proceeds with fast kinetics at both graphite and boron-doped diamond electrodes and may therefore be regarded as the first example of facile electron transfer between diamond and a deposit at the electrode surface owing to good electrical contact at the three-phase boundary.

Acknowledgements F.M. thanks the Royal Society for the award of a University Research Fellowship and New College (Oxford) for a Stipendiary Lectureship. We thank G. Scarsbrook, R.S. Sussmann, and A.J. Whitehead (De Beers Industrial Diamond Division) for making available boron-doped diamond electrode materials.

References

1. Pleskov YuV (1999) Russ Chem Rev 68: 381
2. Swain GM, Anderson AB, Angus JC (1998) MRS Bull 56
3. Goeting CH, Marken F, Gutierrez-Sosa A, Compton RG, Foord JS (1999) New Diamond Frontier Carbon Technol 3: 207
4. Michaud PA, Mahe E, Haenni W, Perret A, Comninellis C (2000) Electrochem Solid State Lett 3: (in press)
5. Okino F, Shibata H, Kawasaki S, Touhara H, Momota K, Nishitani-Gamo M, Sakaguchi I, Ando T (1999) Electrochem Solid State Lett 2: 382
6. Xu JZ, Swain GM (1998) Anal Chem 70: 1502
7. Rao TN, Yagi I, Miwa T, Tryk DA, Fujishima A (1999) Anal Chem 71: 2506
8. Saterlay AJ, Agra-Gutierrez C, Taylor MP, Marken F, Compton RG (1999) Electroanalysis 11: 1083
9. Saterlay AJ, Foord JS, Compton RG (1999) Analyst 124: 1791
10. Katsuki N, Takahashi E, Toyoda M, Kurosu T, Iida M, Wakita S, Nishiki Y, Shimamune T (1998) J Electrochem Soc 145: 2358
11. Fryda M, Herrmann M, Schäfer L, Klages CP, Perret A, Haenni W, Comninellis C, Gandini D (1999) New Diamond Frontier Carbon Technol 9: 229
12. Bouamrane P, Tadjeddine A, Butler JE, Tenne R, Levy-Clement C (1996) J Electroanal Chem 405: 95
13. Xu J, Granger MC, Chen Q, Strojek JW, Lister TE, Swain GM (1997) Anal Chem 69: 591A
14. Vinokur N, Miller B (1996) J Electrochem Soc 143: L238
15. Yagi I, Notsu H, Kondo T, Tryk DA, Fujishima A (1999) J Electroanal Chem 473: 173
16. Compton RG, Marken F, Goeting CH, McKeown RAJ, Foord JS, Scarsbrook G, Sussmann RS, Whitehead AJ (1998) Chem Commun 1961
17. Awada M, Strojek JW, Swain GM (1995) J Electrochem Soc 142: L42
18. Manivannan A, Tryk DA, Fujishima A (1999) Electrochem Solid State Lett 2: 455
19. Vinokur N, Miller B, Avyigal Y, Kalish R (1999) J Electrochem Soc 146: 125
20. Goeting CH, Jones F, Foord JS, Eklund JC, Marken F, Compton RG, Chalker PR, Johnston C (1998) J Electroanal Chem 442: 207
21. Marken F, Webster RD, Bull SD, Davies SG (1997) J Electroanal Chem 437: 209
22. Marken F, Compton RG, Goeting CH, Foord JS, Bull SD, Davies SG (1998) Electroanalysis 10: 821
23. Goeting CH, Foord JS, Marken F, Compton RG (1999) Diamond Relat Mater 8: 824
24. Levy-Clement C, Zenia F, Ndao NA, Deneuville A (1999) New Diamond Frontier Carbon Technol 9: 189
25. Granger MC, Swain GM (1999) J Electrochem Soc 146: 4551
26. Tatawawadi SV, Piekarski S, Hawley MD, Adams RN (1967) Chem Listy 61: 624
27. Ravichandran K, Baldwin RP (1983) Anal Chem 55: 1586
28. Philp RH (1970) J Electroanal Chem 27: 369

29. Marken F, Compton RG, Bull SD, Davies SG (1997) Chem Commun 995
30. Marken F, Blythe AN, Wadhawan J, Compton RG, Bull SD, Aplin RT, Davies SG (2000) J Solid State Electrochem 4: (in press)
31. Adams RN (1969) Electrochemistry at solid electrodes. Dekker, New York, p 361
32. Ball JC, Marken F, Fulian Q, Wadhawan JD, Blythe AN, Schröder U, Compton RG, Bull SD, Davies SG (2000) Electroanalysis (in press)